Nuclear Materials and Energy 19 (2019) 440–444

Contents lists available at ScienceDirect

Nuclear Materials and Energy

journal homepage: www.elsevier.com/locate/nme

Investigation of hydrogen isotope retention mechanisms in beryllium: High resolution TPD measurements

Michael Eichler

Forschungszentrum Jülich GmbH, Institut für Energie- und Klimaforschung - Plasmaphysik, 52428 Juelich, Deutschland, Germany

ARTICLE INFO

Keywords:
Hydrogen retention
Beryllium
Temperature programmed desorption spectrum
Deuterium implantation
Blisters
Low temperature desorption

ABSTRACT

The retention of ion-implanted deuterium in beryllium poly- and single crystals at room temperature is studied using high precision temperature programmed desorption spectroscopy (TPD). Slow temperature ramps of 0.01 K/s in combination with well-defined experimental conditions are used to resolve the low temperature desorption regime for the first time revealing three sharp desorption peaks. The comparison to results of a coupled reaction diffusion system (CRDS) model shows, that the corresponding release mechanisms cannot be described by thermally activated rate processes. SEM images of a polycrystalline beryllium sample after implantation of deuterium with 2 keV per D atom show the formation of blisters of roughly 1 μm in diameter. Additionally, cracks on top of the blisters are found as well as spots, on which blisters are peeled off. Both processes are discussed to play a role in the low temperature release regime of the retained deuterium. Investigation of TPD spectra performed on single crystalline beryllium shows a jagged pattern in the low temperature release regime, which can be connected to blisters bursting up, releasing big amounts of deuterium in short time scales.

1. Introduction

The first wall of the international nuclear fusion experiment ITER will consist to large extent of metallic beryllium [1]. During operation, deuterium and tritium from the plasma will be implanted in plasma facing components (PFC). The retained amount as well as the temperature dependent release of deuterium after implantation is of importance regarding the fuel balance in the plasma and possible changes of physical properties of the materials caused by hydrogen uptake. To predict the behavior of the PFC under the wide range of conditions that are to be expected in a fusion reactor, an understanding of the dominating mechanisms of hydrogen transport in the material and retention after implantation is required. To extract that information on atomic scale, laboratory experiments on hydrogen implantation and release are performed and rate equation simulations are applied to test fundamental parameters, like diffusion coefficients of interstitial atoms and binding energies of hydrogen in different crystal defects, calculated *ab initio* within the density functional theory (DFT) approach, against the experimental results. Besides the quantitative determination of energetic parameters, the comparison of simulation and experiment can indicate the dominating retention and release mechanisms taking place, like hydrogen accumulation on the sample surface.

With this aim, the retention and temperature dependent release of deuterium in beryllium poly- and single crystals under well-defined conditions is studied using the ultra-high vacuum experiment ARTOSS [2]. With this facility, the in situ preparation and analysis of atomically clean surfaces is possible. Comparable measurements have already been done at the same facility, addressing anisotropic diffusivity of self-interstitial Be atoms and fast hydrogen diffusion along grain boundaries in the beryllium single crystal [3–6]. Previous desorption experiments show the appearance of a low-temperature desorption peak around 460 K above implantation fluences of 1E21 m^{-2}. The processes that lead to this desorption peak are not understood yet.

This work aims to investigate the mechanisms resulting in the formation of the low temperature desorption peak. For this, the experimental setup was improved to allow high resolution temperature programmed desorption (TPD), that resolved the low temperature peak and for the first time revealed a set of three sharp desorption maxima. Furthermore, measurement series with different implantation fluences are presented and compared to already existing data [4] and modeling results [7]. In addition, desorption spectra of polycrystalline beryllium and (11–20) oriented single crystal are compared.

2. Experimental setup/procedure

The essential idea is to create very well defined and stable experimental conditions and the opportunity to vary single parameters in order to study the corresponding response of the system to understand

E-mail addresses: m.eichler@fz-juelich.de, m.eichler@fz-juelich.de.

https://doi.org/10.1016/j.nme.2019.03.018
Received 17 August 2018; Received in revised form 1 March 2019; Accepted 20 March 2019
Available online 04 April 2019

basic atomistic mechanisms of retention and release of hydrogen isotopes.

The ultra-high vacuum apparatus ARTOSS combines several surface diagnostics including X-ray photoelectron spectroscopy (XPS) and a quadrupole mass spectrometer (QMS) to perform TPD measurements.

The whole experiment is carried out in situ with a base pressure < 4E-11 mbar to ensure a clean sample surface over several hours. After each experiment, the sample is cleaned by 5 keV Ar sputtering with a fluence of 4E21 Ar/m^2 to remove the oxygen layer and other possible impurities, as well as an approx. 100 nm thick layer of the beryllium surface, which includes the implantation zone of the previous experiment, that could be subject to heavy structural changes. Afterwards, the sample is annealed to 950 K for 30 min to heal out defects in the crystal caused by the sputtering process. After the cleaning procedure, the oxygen coverage of the surface is verified by XPS to be less than 0.2 ml and the sample can be reused for the next experiment.

For the implantation of deuterium, D_3^+ ions are accelerated towards the sample with 4 kV, while the sample is grounded via Zener diodes, which allow the current to flow when 1 kV on the sample is reached. Thus, the potential of the sample is formed due to the implanted ions, and can be maintained for implantation currents > 0.1 μA, resulting in an implantation energy of 1 keV per D atom. As a positive potential of 1 kV is applied to the sample, secondary electrons are attracted and taken into account for the current measurement while secondary ions are repelled and hence missed. To ensure energy and mass separated implantation of D_3^+, the ion beam is deflected by 60° using a bending magnet before guiding to the surface. Using the described setup, an implantation current of 2.5 μA can be achieved which equals a flux of 1E18 m$^{-2}s^{-1}$.

During implantation, sample temperature rises 5 – 7 K from room temperature. A total rectangular area of 45 mm^2 on the beryllium sample is irradiated by placing an array of 12 sequential implantation spots, 3 (horizontal) and 4 (vertical), in the distance of the FWHM of each of those spots. The implantation spot is of elliptical form with a FWHM of 1.5 mm and 2.5 mm along the vertical and horizontal axes respectively. The disadvantage of this method is the different "age" of each implantation spot before TPD, which depends on the implantation flux and fluence and can vary from seconds in case of the last spot to hours regarding the first spot. That only shows an effect on beryllium samples for fluences > 1E21 m^{-2} (see Fig. 1). The remaining surface of the sample is used to spot-weld two thermocouple wires as well as a wire to ground the sample and measure the current originating from the ion implantation.

Particles released from the sample surface are guided through a gold-coated "snorkel" towards the sequentially pumped QMS (Balzers QMA 422). This way, the system responds faster to varying outgassing behavior of the sample. The sample holder is equipped with an electron impact heater connected to a PID controller. The sample temperature responds to a change in heating power in < 1 s due to low heat capacity of the thin sample (0.5 mm). The temperature is measured with 50 Hz sampling rate and a resolution of 0.001 K.

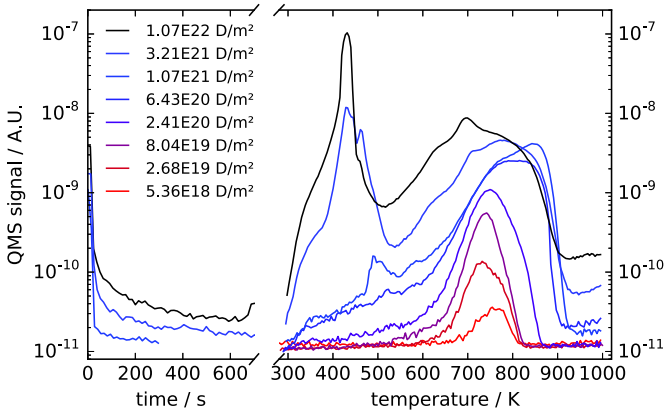

Fig. 1. TPD spectra and outgasing after implantation of D_3^+ ions at 1 keV/D and various fluences in polycrystalline Be at room temperature. Temperature ramp: 0.3 K/s. The formation of the "low temperature" desorption peak starts at a fluence of 1E21 m^{-2}.

The described features allow stable and accurate linear heating ramps between < 0.005 K/s and 20 K/s. For most of the presented experiments, a ramp with 0.01 K/s is chosen. Deviations from the desired heating rate are smaller than 0.001 K/s.

Using such slow temperature ramps, the temperature gradient across the sample surface is dependent on the sample temperature and is < 2 K/cm for a sample temperature of 1000 K, while the temperature deviation across the implantation spot is < 1 K. The values were estimated by finite element analysis of the sample holder and manipulator. In fact, the peak positions in desorption spectra can be reproduced with an accuracy of about 1 K within a repetitive measurement series. However, when the thermocouple on the sample surface needs to be renewed, e.g. as a consequence of a burned heating filament, the desorption peak positions can deviate up to 20–30 K. For this reason, relative shifts of desorption peak positions can only be compared within uninterrupted measurement series.

3. Retention measurements

3.1. Fluence scan of polycrystalline beryllium

Fig. 1 shows a series of TPD spectra of deuterium implanted in a beryllium poly-crystal at 1 keV per D atom and different fluences starting from 5E18 m^{-2} up to 1E22 m^{-2}. After the implantation process of each measurement, the linear heating ramp of 0.3 K/s is started after 650 s waiting time. For fluences smaller than 1E21 m^{-2}, the deuterium signal in the chamber drops to the background noise directly after closing the shutter of the ion beam at $t = 0$ s. However, for fluences of 1E21 m^{-2} to 1E22 m^{-2}, dynamic outgassing after the implantation is observed, which is shown in the left part of Fig. 1, suggesting that not all implanted deuterium can be accommodated at material defects produced during the implantation. At the same time, starting from 1E21 m^{-2} the low temperature desorption peak occurs at roughly 500 K shifting to lower temperatures for higher fluences. The high temperature desorption peak is located between 700 K and 800 K for low fluences, developing a shoulder to 850 K above 2E20 m^{-2} that dominates the spectrum at 1E21 m^{-2}. For higher fluences and with the growth of the low temperature peak, the peak at 850 K vanishes. For the highest measured fluences, the deuterium signal does not drop to the background level even at 1000 K, which can be due to deeper diffusion of deuterium into the bulk.

By integration of the spectra, the total amount of retained deuterium is obtained, which is shown in Fig. 2. For comparison, already existing data from [8] and [9] is plotted as well. The data of our work is not absolutely calibrated. Instead, it is scaled so that low fluence retention values match to literature data, part of which was measured at the ARTOSS facility as well. The relative change of absolute retention values at different fluences within our fluence scan is consistent since the operation settings of the QMS were not changed and the pumping speed was kept constant for all measurements in the series. Changes in detector sensitivity are monitored by conducting TPD experiments using identically prepared samples.

In previous experiments reported in the literature [8], retention saturated for fluences above 1E21 m^{-2}, which was also connected to the formation of the low temperature desorption peak. However, the fluence scan of our work shows saturation at roughly 1E22 m^{-2}. Despite the fact, that the QMS is not absolutely calibrated and the implantation current measurement is not corrected for secondary ions, the measured fluences are comparable to previous experiments, as well as the threshold fluence for the formation of the low temperature

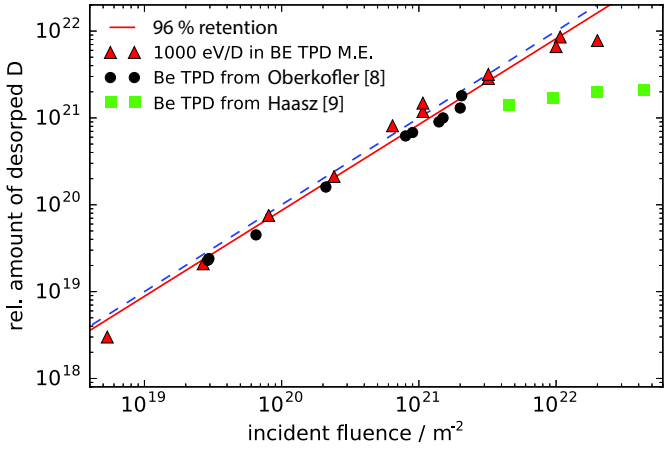

Fig. 2. D retention in polycrystalline Be as function of D ion fluence. Black data points [8], green data points [9]. Red data points, our work – without absolute calibration. The blue line represents 100% retention. Implantation at room temperature and 1 keV per atom. (For interpretation of the references to color in this figure legend, the reader is referred to the web version of this article.)

desorption peak. To match the saturation fluence with previous experiments, a mismatch of the measured implantation beam current by a factor of 10 is needed, which can be excluded for the performed measurements. Such a correction, in particular, would result in a shift of the threshold fluence for the formation of the low temperature peak to 1E20 m^{-2}, inconsistent with previous studies. The delayed saturation can be related to the shape and scanning procedure of the ion beam. Part of the total implanted area gets less fluence and comes to saturation later. In particular in the case of earlier high fluence ARTOSS exposures [3] the distribution of the implanted fluence over the exposed area was difficult to control and quantify.

3.2. High resolution TPD spectra

As described in Section 2, the sample heating system is refined to allow linear temperature ramps of 0.01 K/s. In Fig. 3, the influence of different heating rates on the desorption spectrum of deuterium from a beryllium poly-crystal is shown. While the fine structure of the low temperature peak is not visible using a temperature ramp of 0.3 K/s, already two desorption peaks and a shoulder between them can be resolved using a 0.05 K/s ramp. With a 0.01 K/s temperature ramp minimum 3 desorption peaks in the low temperature domain can be

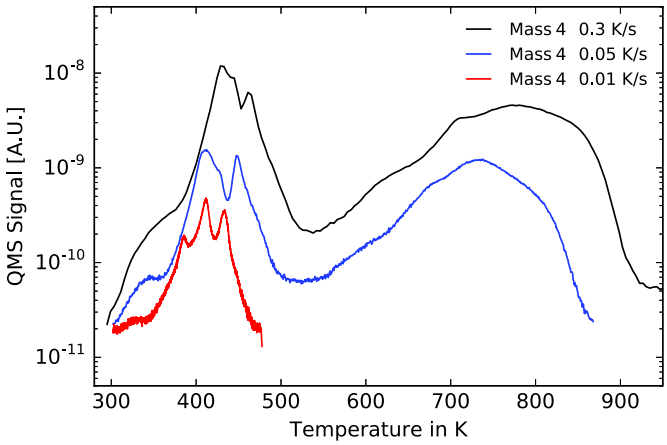

Fig. 3. TPD spectra after implantation of D_3^+ ions with a fluence of 3.2E21 m^{-2} at 1 keV/D in polycrystalline Be at room temperature with temperature ramps of 0.01 – 0.3 K/s. Slower temperature ramps (0.01 K/s) reveal multiple “low-temperature” desorption peaks.

separated. The signal to noise ratio of the QMS measurement is reduced for slower heating rates, as the same amount of deuterium is released in longer time periods, which is a factor of 30 reduction between 0.3 K/s and 0.01 K/s. The spectrum for 0.01 K/s was aborted at 480 K due to technical issues.

As a first attempt to examine the recorded spectra, the activation energies of desorption for the 3 distinct desorption peaks in the low temperature regime are determined using Redhead's peak maximum method [10] with a variation of the heating rates. In this approach, the desorption is regarded as a single step temperature activated process, de-trapping, diffusion and recombination are not separated. Using this method, activation energies of 0.43 eV, 0.67 eV and 0.82 eV were deduced for the three low temperature peaks starting from lower to higher release temperature.

To understand and reproduce the features of the recorded spectra, the reaction-diffusion model CRDS [7] is used. In this model, processes of trapping/de-trapping, diffusion and desorption are all taken into account in a system of coupled partial differential equations. One possible interpretation of the low temperature desorption regime would be desorption of deuterium accumulated on the sample surface after the bulk trapping sites are saturated. However, this assumption is in contradiction with the integral D amount attributed to the low temperature peak. To address this issue, an extended surface area has been assumed in [7], e.g. due to porosity, so that the effective surface area is at least factor 10 larger than the nominal implanted area. In such a way the formation and evolution of the low temperature desorption peak can be qualitatively explained, but it was pointed out that the shape of the low temperature peak resulting from simulations does not reflect that seen in experiments. New observations with the high resolution TDS question the model assumptions further.

CRDS simulations for a simplified system where only deuterium at the surface with either first or second order desorption process is considered cannot reproduce the low temperature desorption peak. As it is also known from the literature [11], surface desorption peak appears to be significantly broader than observed in our experiments. Considering 3 different surface adsorption sites with experimentally determined desorption activation energies does not result in resolvable peaks. Full width at half maximum (FWHM) of the simulated single peak is about 50 K while experimental peaks have FWHM less than 20 K.

In the second approach, bulk retention with 3 different trapping sites is considered. Fast diffusion to the surface and immediate recombination are imposed. Using experimentally determined activation energies for de-trapping and adjusting the de-trapping frequency, narrow desorption peaks cannot be reproduced. While using a reasonable value for the de-trapping frequency, e.g. 1E13 s^{-1}, de-trapping energies have to be adjusted to 1.22 eV, 1.30 eV and 1.37 eV to match the peak maxima to the experimental data. However, in this case it is not possible to reproduce sharp desorption peaks as seen in the experiment (Fig. 4).

A possible mechanism for such a narrow desorption peak would be strongly surface-limited desorption from the bulk, in which the surface is saturated with D atoms and the D source in the bulk is sufficient to replenish the surface to balance the recombination and respective desorption. This assumption implies a situation when transport of solute D atoms to the surface is limited by recombination leading to their diffusion and uniform distribution throughout the entire sample, which seems to be not very realistic. Further investigations of that kind are ongoing to resolve the discrepancies between experiment and modeling, and surface morphology changes after implantation might give an indication of mechanisms at play.

3.3. SEM pictures of D implanted Be sample

The decomposition of BeD_2 during temperature desorption spectroscopy, which can be formed during implantation and which was actually detected on one Be poly-crystal, is discussed as a candidate

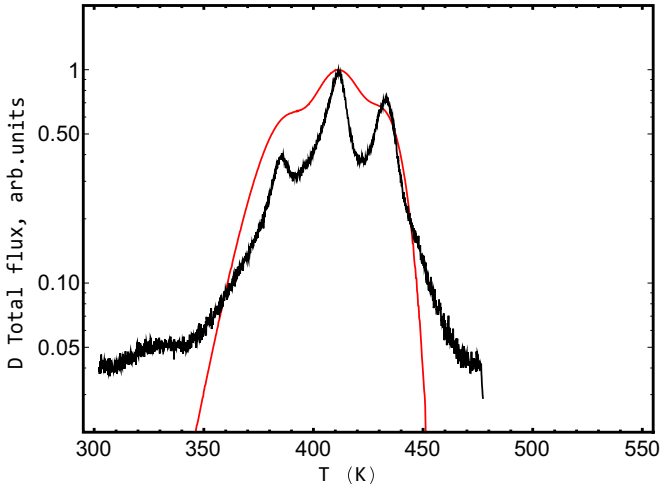

Fig. 4. Comparison of normalized measured TPD spectrum using a 0.01 K/s heating ramp and simulated TPD spectrum using CRDS. The implantation fluence is 3. 2E21 m^{-2} at 1 keV/D in polycrystalline Be at room temperature. The simulation includes 3 different trap sites with energies 1.22 eV, 1.30 eV and 1.37 eV, fast diffusion and immediate recombination.

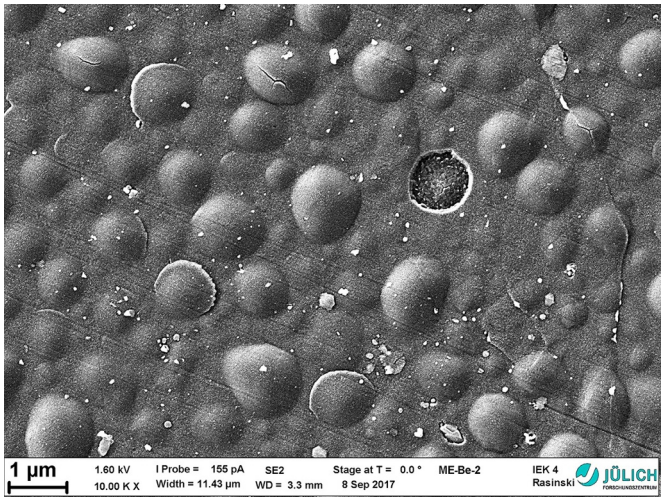

Fig. 5. SEM image of a beryllium polycrystal after implantation of D_3^+ ions at 2 keV/D. Blisters are formed on the surface, which are partially cracked open on the top while others are peeled off or in the process to flake.

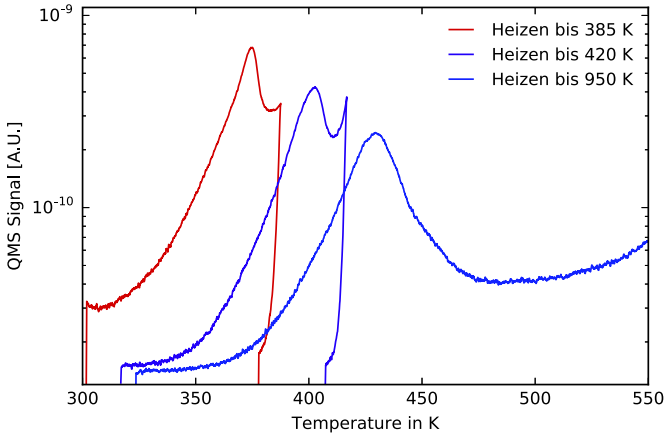

Fig. 6. Low temperature desorption peak of polycrystal after D implantation with a fluence of 3.2E21 m^{-2} at 1 keV/D: Heating is stopped after each desorption peak and started again after sample is cooled down to approx. 320 K. A temperature ramp of 0.01 K/s is chosen.

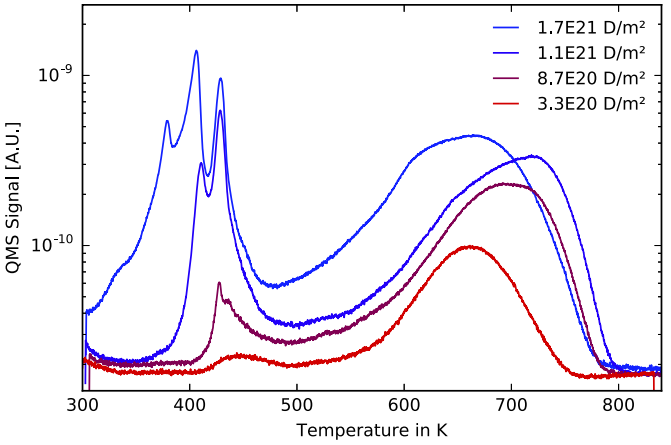

Fig. 7. TPD spectra after implantation of D_3^+ ions at 1 keV/D and various fluences (formation of "low temperature" peak) in polycrystalline Be at room temperature. Temperature ramp: 0.01 K/s.

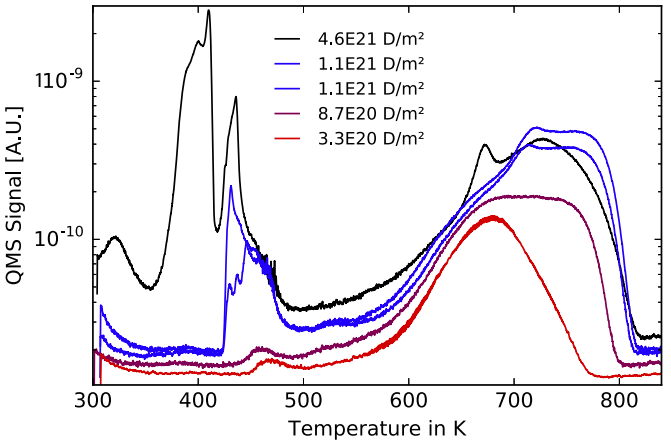

Fig. 8. TPD spectra after implantation of D_3^+ ions at 1 keV/D and various fluences (formation of "low temperature" peak) in single-crystalline Be at room temperature. Temperature ramp: 0.01 K/s.

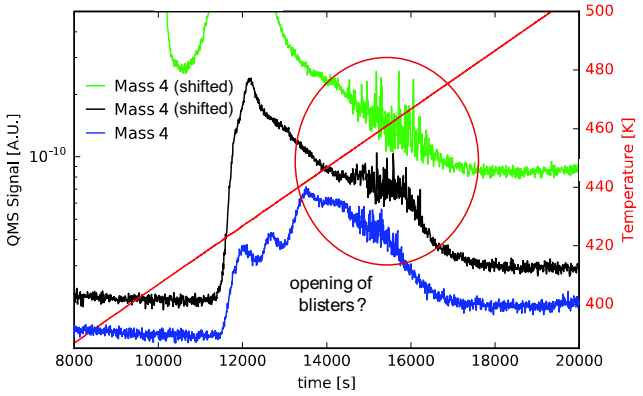

Fig. 9. Low temperature desorption peak of single crystal after implantation of D with a fluence of 1.1E21 m^{-2} at 1 keV/D: The marked pattern occurs on both identical measurements and might be caused by the opening of blisters on the beryllium surface.

mechanism for the desorption peak at low temperatures [12]. To verify the proposed mechanism, the very beryllium sample that was used in [12], was prepared in a similar way and exposed to a 6 keV D_3 ion beam (2 keV per atom). Several implantation spots were loaded with different fluences ranging from 1E20 m^{-2} up to 1E23 m^{-2}. Afterwards, the

sample was analyzed by SEM. BeD_2 structures reported in [12] could not be detected. Instead, blisters of approx. 1 μm in diameter were found on the beryllium surface, as shown in Fig. 5. The blister density grows with the implantation fluence, which is a proof, that the blister formation is directly connected to the implantation of deuterium. Low temperature desorption is observed without presence of BeD_2 crystallite structures on the surface. On top of some blisters, small cracks are visible, some other blisters are about to flake. A small fraction has already peeled off. The formation of blisters due to implantation allows for a speculation, that the low temperature desorption regime with its relatively sharp peaks is connected to blisters breaking up and releasing larger amounts of molecular deuterium in a single event or frequent event series.

Further experiments have been conducted to validate and understand the mechanisms behind the formation of the three low temperature desorption peaks.

To understand, if deuterium in the three different (hypothetical) trapping sites attributed to three peaks is interchangeable, the beryllium sample was prepared according to the standard experimental procedure described in Section 2 with a fluence of 3.2E21 m^{-2} and, instead of performing a full TPD spectrum from room temperature to 950 K, the heating was aborted after the first desorption peak. The heating process was started again after the sample was cooled down to nearly room temperature, which took approximately 30 min, and aborted again after the second desorption peak. Finally the same procedure was performed for the third release peak. As shown in Fig. 6, the trapping sites depleted in one of the heating steps are not refilled before or during the subsequent step. This observation suggests that deuterium is not mobile until de-trapping occurs, thus reducing the credibility of the strongly surface-limited release hypothesis mentioned earlier. Further experiments using different isotopes (H, D) will be performed to study exchange effects between different trapping sites.

3.4. High resolution TPD of Be single crystal

To investigate a possible influence of different crystal orientations, a comparable fluence scan as for the poly-crystal described in Section 3.1 was performed on a beryllium single crystal. The fluence steps were chosen to picture the formation of the low temperature peaks in detail. Figs. 7 and 8 show the fluence scans at comparable fluences for the polycrystalline Be and Be single crystal respectively. Note that Fig. 8 contains two measurements at the same fluence of 1.1E21. In comparison to the poly-crystal, several conclusions can be drawn. The low temperature peak is less pronounced relative to the high temperature desorption peak in the single crystal in comparison to the poly-crystal. Furthermore, the desorption regimes are shifted to higher temperatures in case of the single crystal that, however, could be caused by a worse connection of the thermocouple as it was clamped instead of spot-welded for this measurement series. The effect of shifted desorption temperatures for single crystals in comparison to poly-crystals has already been discussed e. g. in [6]. The features of the low temperature desorption as well as of the high temperature desorption peaks are even sharper and more pronounced compared to the poly-crystal. The low temperature desorption peak of the single crystal has an extremely steep leading edge, which de facto excludes typical thermally activated process as responsible mechanisms.

In Fig. 9, the low temperature parts of two TPD spectra obtained for identical fluence of 1.1E21 m^{-2} and one spectrum obtained for a fluence of 4.6E21 m^{-2} from the single crystal are plotted. Two of the spectra are shifted along the vertical axis for a better visualization (the actual non-shifted background levels in the time interval from 8000 s to 11000 s do lie on top of each other). Despite the fact, that the spectrum for identical fluence is not reproduced, a noisy pattern appears in all cases at the same temperature. To demonstrate that such a pattern is not an artifact of unstable temperature control, the temperature ramp is plotted as well. With the temperature ramp being absolutely stable and smooth in both experiments, the measured effect originates from the sample. A possible explanation for the pattern is the massive escape of deuterium molecules from blisters after their break-up due to temperature increase. Note, that a similar effect is not visible on TPD spectra of the polycrystalline beryllium sample. What mechanism is causing the noisy pattern and how it can be connected to the single crystal and the low temperature desorption peaks is still on a level of speculation and further investigation is required to create a consistent theory.

4. Summary

The ultra-high vacuum experiment ARTOSS has been updated and revised to allow reproducible high precision thermal desorption experiments. TPD spectra of deuterium implanted into poly- and single-crystalline beryllium with a wide range of fluences have been recorded, visualizing the evolution of retention. It has been demonstrated that using slow temperature ramps for TPD spectroscopy can give additional information about the release mechanisms of retained species in a material. In the case of beryllium, the low temperature peak was for the first time resolved to consist of three sharp desorption peaks. SEM pictures were taken of a beryllium poly-crystal after implantation of deuterium with several fluences, showing the formation of blisters being a probable candidate to explain the low temperature desorption regime.

Acknowledgments

This work has been carried out within the framework of the EUROfusion Consortium and has received funding from the Euratom research and training programme 2014–2018 under grant agreement No 633053. The views and opinions expressed herein do not necessarily reflect those of the European Commission.

Work performed under EUROfusion WPPFC.

References

[1] M. Shimada, D.J. Campbell, V. Mukhovatov, M. Fujiwara, N. Kirneva, K. Lackner, M. Nagami, V.D. Pustovitov, N. Uckan, J. Wesley, N. Asakura, A.E. Costley, A.J.H. Donné, E.J. Doyle, A. Fasoli, C. Gormezano, Y. Gribov, O. Gruber, T.C. Hender, W. Houlberg, S. Ide, Y. Kamada, A. Leonard, B. Lipschultz, A. Loarte, K. Miyamoto, V. Mukhovatov, T.H. Osborne, A. Polevoi, A.C.C. Sips, Nucl. Fusion 47 (2007) S1.
[2] Ch. Linsmeier, P. Goldstraß, K.U. Klages, Phys. Scr. T94 (2001) 28.
[3] M. Reinelt, A. Allouche, M. Oberkofler, Ch. Linsmeier, New J. Phys. 11 (2009) 043023.
[4] M. Oberkofler, M. Reinelt, Ch. Linsmeier, Nucl. Instrum. Meth. B 269 (2011) 1266.
[5] M. Oberkofler, M. Reinelt, A. Allouche, S. Lindig, Ch. Linsmeier, Phys. Scr. T138 (2009) 014036.
[6] M. Oberkofler, M. Reinelt, S. Lindig, Ch. Linsmeier, Nucl. Instrum. Meth. B 267 (2009) 718.
[7] D. Matveev, M. Wensing, L. Ferry, F. Virot, M. Barrachin, Y. Ferro, Ch. Linsmeier, Nucl. Instrum. Meth. B 430 (2018) 23.
[8] M. Oberkofler, Rückhaltemechanismen für Wasserstoff in metallischem Beryllium und Berylliumoxid sowie Eigenschaften von ioneninduziertem Berylliumnitrid, 2011.
[9] A.A. Haasz, J.W. Davis, J. Nucl. Mater. 241–243 (1997) 1076.
[10] P.A. Redhead, Vacuum 12 (1962) 203.
[11] V. Lossev, J. Küppers, Surf. Sci. 284 (1993) 175.
[12] C. Pardanaud, M.I. Rusu, C. Martin, G. Giacometti, P. Roubin, Y. Ferro, A. Allouche, M. Oberkofler, M. Köppen, T. Dittmar, Ch. Linsmeier, J. Phys. Cond. Matter 27 (2015) 47.